SLAC-PUB-1882
February 1977
(T/E)

A MODEL FOR MASSIVE LEPTON PAIR PRODUCTION*

M. Duong-van, K. V. Vasavada,† and R. Blankenbecler
Stanford Linear Accelerator Center
Stanford University, Stanford, California 94305

ABSTRACT

A general model for the production of massive lepton pairs is discussed with emphasis on the predicted distributions of mass, transverse, and longitudinal momentum. A comparison with proton-proton experiments is given and the fit is satisfactory for all three distributions. The model is essentially the CIM approach to large transverse momentum reactions and no new parameters are needed. In a specific kinematic limit, it predicts the same mass distribution as the Drell-Yan model.

(Submitted to Phys. Rev.)

*Work supported by the Energy Research and Development Administration.
†Present address: Physics Department, Indiana-Purdue University, Indianapolis, Indiana 46205.

I. INTRODUCTION

Since the original proposal by Lederman,[1] the study of massive lepton pair production has generated considerable experimental and theoretical interest. The most successful theoretical model for this process is the parton approach developed by Drell and Yan.[2] For a recent review of this general subject, see Ref. 3. The observation of an anomalously large yield of prompt single leptons by the Chicago-Princeton group,[4] has further generated interest in the pair yield[5,10] and possibly new (unidentified) sources.

The recent observation[6,7,8,9] of a large average transverse momentum for the virtual photon in massive lepton pair production has likewise generated a renewed interest in the basic theory.[10] In the usual Drell-Yan (D-Y) picture of this reaction, the photon is directly produced by the annihilation of a quark-antiquark pair. Therefore a large P_T of the photon must be due to large P_T components in the initial state quark and/or antiquark wave functions. Such large P_T values, however, can raise difficulties in the interpretation of other experiments.

In this note, we wish to expand on a more general model of massive di-lepton production that was described earlier[11,12] and apply it to proton-proton collisions. In this approach the photon is produced in a scattering process, not via annihilation, and the large transverse momentum arises therefrom. The large P_T is not to be thought of as characteristic of the initial state but rather as characteristic of the final state. Different final states have different P_T distributions in our theory. The model used here is an application of the CIM model[13] of large P_T to large mass production. We shall make no new assumptions and the results derived here are just those of the CIM. Since our model of massive lepton pair production is basically the same as the CIM model of large P_T hadron production, one predicts that the large P_T single lepton rate should behave essentially like the large P_T pion rate. The model predicts slight differences, however, and the lepton/pion ratio should rise as $\sim p_T^2$. A rise is observed[4]. The model described here is a unified approach to lepton pair and hadronic production. We shall discuss only the continuum, but an extension to the production of the new particles is possible. Since low mass photons can come from many sources, for example meson-pair annihilation, and these are neglected here, we expect our model to fall below the data at low photon mass, or Q, values.

As was stressed in the original discussion of the D-Y model, the annihilation graph is gauge invariant only if both the quark and antiquark are on-shell; additional graphs are not then necessary. The narrow transverse momentum distribution of the model assures that this is a good approximation. However, the photon then is restricted to have a very small average transverse momentum $< Q_T >$. If one arbitrarily broadens the distribution functions of the initial pair, several difficulties arise: gauge invariance is no longer guaranteed because the quarks are forced to be far off-shell, there are problems in avoiding double counting and in keeping the correct final state coherence properties in any hard scattering model of the parton type; finally, as will be discussed later in detail, there would be severe difficulties in interpreting inclusive hadron experiments at large p_T. In a sense, the model presented here is one of the simplest that avoids the above difficulties yet allows the photon to be produced at large Q_T.

This model also allows us to normalize the predicted rate in two different ways. One way is a fit to the measured antiquark distribution functions, as in the D-Y model, and a second method is a fit to the large p_T production of mesons. These methods yield compatible rates within the uncertainties. Another way of stating this result is that in our model, the measured antiquark distribution functions fix the rates of production of massive lepton pairs and large p_T mesons. These two reactions are related in our model because the (sea) antiquarks are assumed to arise predominantly from the decay of virtual mesons not from gluons. This is natural because they are the lightest intermediate states available that are strongly coupled.

It has been argued in Ref. 11 that the CIM model should be applicable not only to large p_T processes but also to large mass production. The present application is therefore a very natural union of these two regimes. Even though our model looks different from the Drell-Yan model, it will be shown that annihilation terms dominate in the limit of large photon mass Q at fixed Q_T. Unlike the D-Y model however, the Q_T distribution is broad. At fixed Q, and large Q_T, the D-Y term is cancelled (this is guaranteed by gauge invariance in the model) and the remainder is consistent with the CIM predictions. The main new feature of our model is that since the photon is produced in a scattering process, the Q_T distribution is power behaved and its width involves Q instead of just the typical transverse momenta fluctuations of the initial state as in the original D-Y model.

II. THE MODEL

We will use the formalism originally devised to describe hard scattering models, and applied especially to the large transverse momentum regime. Following the notation of Ref. 11, as illustrated in Fig. 1, the fully differential cross section is

$$\begin{aligned} R(A,B) &\equiv Q^4 \frac{d\sigma}{dQ^4}(AB \to \ell^+\ell^- X) \\ &= \sum_{a,b,d} \int dx\, d^2k_T\, dy\, d^2\ell_T\, G_{a/A}(x,k_T)\, G_{b/B}(y,\ell_T) \\ &\qquad \otimes R(a,b;d) \end{aligned} \tag{1}$$

where

$$R(a,b;d) = Q^4 \frac{d\sigma}{dQ^4} (ab \to \ell^+\ell^- d) \tag{2}$$

and trivial kinematic offshell effects have been neglected. R is assumed to be onshell and is evaluated at reduced values of s, t, and u.

We now choose the dominant basic process to be inverse photoproduction, meson-quark $\to$ "photon"-quark, as illustrated in Fig. 2. This is the direct analogue of the process used to describe large P_T reactions producing mesons. The first term, the u-pole, clearly involves $\bar{q}$+q annihilation and will be shown to be closely related to the D-Y process in a certain limit.

Corrections from this term, as well as the s-pole, will not scale in the large Q limit but will be important in the large Q_T limit. Our interest here is to describe general kinematic effects and not detailed angular distributions, opposite side correlations, etc. Therefore, the simplest quark model will be adopted—a renormalizable theory of scalar quarks with a $\lambda\phi^4$ interaction. Neglecting the pion mass and denoting the quark mass by M, the basic cross section achieves a simple form after summing over the lepton spins:

$$R(M,q;q) = \frac{1}{6\pi^2} \alpha^2 h^2 \, \delta(s'+t'+u'-Q^2-2M^2) \, \Sigma(s',t',u';Q^2) \tag{3}$$

where

$$s'\Sigma = \frac{\lambda^2(u',Q^2,M^2)}{(M^2-u')^2} + \frac{\lambda^2(s',Q^2,M^2)}{(s'-M^2)^2} + \frac{2}{(s'-M^2)(M^2-u')} \left[2Q^2(s'-Q^2+u') + (s'-Q^2-M^2)(u'-Q^2-M^2)\right] \tag{4}$$

and

$$\lambda^2(a,b,c) = a^2+b^2+c^2-2(ab+bc+ca) \quad .$$

The variables s', t', and u' describe the basic process and will be related to the external variables s, t, u by simple kinematics. The coupling of the (composite) mesons to the quarks is denoted by h^2.

The dimensional counting form of structure functions in renormalizable theories, including both the x and k_T behavior, has already been given.[14] An approximate form having the correct behavior in all limits is (see Fig. 1)

$$G_{a/A}(x, k_T) = G_0 (1-x)^g \left[k_T^2 + M^2(x)\right]^{-1-g} , \tag{5}$$

where

$$M^2(x) = a^2(1-x) + \alpha^2 x - x(1-x)A^2 ,$$

and g is given by the usual counting results. Thus the k_T falloff is related to the $x \sim 1$ behavior and $\langle k_T^2 \rangle = M^2(x)/(g-1)$, and depends on x. Since typical interesting values of g are 3, 5, and 7, the average transverse momentum from this source is not large for reasonable mass values.[10] In order to handle the multiple integrations, we will be forced to neglect the k_T distribution in the G's and replace them by delta functions. Their effects can be added to our calculation of $\langle Q_T \rangle$ but their contribution will turn out to be small. A consistency check is that this small additional term be essentially independent of Q^2 and Q_L^2, the longitudinal momentum; the initial state cannot know about the final state except through the slow x-dependence of the k_T^2 width.

In order to get a feeling for the kinematics, consider the limit in which s and Q^2 are large compared to proton and quark masses. One then finds

$$\begin{aligned} s' &= xys \\ t' &= xt + (1-x)Q^2 \\ u' &= yu + (1-y)Q^2 , \end{aligned} \tag{6}$$

and Eq. (1) takes on a definite and simple form. Let us now turn to the distributions predicted by the model.

III. DISTRIBUTIONS

In order to compute the mass distribution, we must integrate over d^4Q at fixed Q^2. The delta function in $R(M,q;q)$ that puts d^2 onshell then fixes $|\vec{Q}|^2$ so that only an angular integral must actually be carried out. One finds in the large s and Q^2 limit:

$$Q^4 \frac{d\sigma}{dQ^2} = 2 \cdot \int dxdy\, G_{M/p}(x)\, G_{q/p}(y)\, r(xys, Q^2) \tag{7}$$

where

$$r(s', Q^2) = Q^4 \frac{d\sigma}{dQ^2}(Mq \to \ell^+\ell^- q) \quad .$$

The factor of two arises from the a=M, b=q and a=q, b=M terms. A simple calculation shows that

$$r(s, Q^2) \cong \frac{1}{12\pi} \alpha^2 h^2 \frac{\epsilon}{s} \left\{ \frac{Q^4}{M^2 s} + \epsilon^2 + 2\left[\frac{Q^2(1+\epsilon)}{s\epsilon} \ln \frac{M^2+s\epsilon}{M^2} - \frac{Q^2}{s} - \frac{1}{2}\right]\right\} ,$$

where

$$\epsilon = 1 - Q^2/s$$

and the order of terms in Σ have been retained. If this is inserted into Eq. (7), with G's of the form

$$G(x) = G_0(1-x)^g/x \quad ,$$

then by using dimensional counting for the structure functions,[14] $g_M=5$, $g_q=3$, one finds

$$R(p,p) \propto h^2 \left[\frac{\epsilon^{11}}{M^2} + \frac{\epsilon^{13}}{Q^2} + O\left(\frac{1}{Q^2}\right)\right] \quad . \tag{8}$$

Therefore the u-pole leads exactly to the Drell-Yan form. All the terms obey the counting rules of Ref. 11.

The reason that the u-pole exactly produces a Drell-Yan term is easily seen. The structure function for a $\bar{q}$ quark contains an explicit contribution in which the antiquark arises from an intermediate virtual meson state[15]:

$$G_{\bar{q}/p}(x) = \int_x^1 \frac{dw}{w}\, G^I_{\bar{q}/M}(x/w)\, G_{M/p}(w) + \ldots \tag{9}$$

The integration over the u-pole diagram contributes a factor $\sim (h^2/M^2)(1-x/w)$ which is the dimensional counting result for $G^I_{\bar{q}/M}$. Thus the ϵ powers in Eq. (8) must agree with dimensional counting as applied to the Drell-Yan process. The Q^2 powers agree automatically for $Q_T \ll Q$.

There are two independent ways to normalize the model. Equation (9) allows us to normalize the model in terms of the fraction of antiquarks that arise from all the possible mesonic intermediate states. In fact, we will assume that <u>all</u> antiquarks arise in this manner and explore the consequences,[16] although more data and a detailed fitting may force a relaxation of this choice. The form of the result (8) implies another self-consistency constraint on the parameters h^2 and M^2. The normalization of the Drell-Yan term depends upon the ratio h^2/M^2. The width of the Q_T distribution will depend on M^2 while the corrections to the D-Y term which are important at small Q^2 are proportional to h^2. Finally, a second and completely independent determination of h^2 and M^2 can be made by fitting large transverse momentum production of mesons since that depends on the basis process ($Mq \to Mq$). This will be done later, but the value of h^2 is found to be consistent between these separate experiments, and we will use $M^2=1$.

The large transverse momentum limit, $Q_T^2 >> Q^2$, is quite different from the above. In this limit, both t' and u' grow as Q_T^2, and the basic cross section becomes

$$s'\Sigma \sim (1-2Q^2/u') + (1-2Q^2/s') + 2\left[-1 - Q^2\,\frac{s'+u'}{s'u'}\right] \sim 4Q^2(s'+u')/(-s'u') \quad .$$

The term that led to the Drell-Yan contribution in the large Q^2 limit explicitly cancels in the large Q_T^2 limit. In a sense, this is guaranteed by the gauge invariance of the basic model amplitude. The basic differential cross section, σ_B, is proportional to Σ/s', and

$$\frac{d\sigma_B}{dQ_T^2} \propto \frac{Q^2(s'+u')}{s'^3(-u')} \sim \frac{1}{s'^3} f(\theta) \tag{10}$$

as is required by dimensional counting[17] for exclusive scattering processes. Note that this result would not have followed if the Drell-Yan term had not cancelled. It immediately follows that for the full inclusive cross section, for $Q_\perp^2 >> Q^2$.

$$R \sim Q_T^{-6} \quad , \tag{11}$$

while for $Q_T \ll Q$, $R \sim Q_T^{-4}$. Let us now turn to a numerical evaluation of the predictions of the model.

IV. NUMERICAL RESULTS

In this note we are considering incident proton beams only. The pion beam case is a very interesting one and numerical results will be presented later. The distribution functions are chosen to be the same as those used to fit electron scattering and large transverse momentum processes. The quark distribution is taken from Ref. 5 but modified at small x to agree with large energy muon scattering. This modification has no effect on the large mass and transverse momentum distributions. The meson distribution is chosen to be

$$G_{M/p}(x) \propto (1-x)^2 G_{q/p}(x) \quad .$$

The overall constants will be chosen shortly. The mass M^2 is chosen to be the same as found in fits to large transverse momentum reactions, $M^2 \simeq 1$. With all the parameters now fixed, let us compute and compare the predictions of the model to experimental data for reasonably large transverse momentum.

Note again that the model requires the presence of two terms from Eq. (1). If a = meson and b = quark, then one must also have the $t \leftrightarrow u$ term where a = quark and b = meson. In the calculations, mass terms were not neglected in the kinematics. Their effect is to slightly smooth the distributions for small Q and Q_T (say < 1).

A. Mass Distribution

First let us compare the mass distribution from the meson-quark (M-q) model with the D-Y model and data. This comparison is given in Fig. 3 at y=0 and $\sqrt{s} = 27.4$. The calculation of the (M-q) curve was based upon an evaluation of $G_{\bar{q}/p}$ using Eq. (9), and then a fit to the measured antiquark distribution functions (from deep inelastic neutrino data).

The normalization condition used above determines the value of h^2. One then predicts the differential cross section for meson-quark scattering at 90° to be

$$\frac{d\sigma}{dt}(Mq \rightarrow Mq) = C/s^4 \quad ,$$

where $C \simeq 1.2 \times 10^3\ (\mathrm{GeV})^4$. From a fit to large P_T production of mesons,[18] the value of C was determined to be $C \approx 10^3\ (\mathrm{GeV})^4$, where the experimental and theoretical uncertainties in this number are at least a factor of 2. This close agreement between the value of h^2 determined by two very different experiments is somewhat fortuitous but is evidence in favor of the meson-quark model. We shall use the former value of C in all the calculations.

We have also compared our absolute prediction with the data of Binkley et al.[6] which is in the range $x_F > 0.2$ and $\sqrt{s} = 23.8$. The agreement with the mass distribution in the range $1.1 < Q < 2.5$ GeV is good. Our prediction is approximately a factor of two higher than the standard D-Y prediction (5) because of the modification at small x of the structure functions mentioned earlier.

B. Transverse Distribution

$\underline{Q_L = 0}$: A comparison with the data of Hom et al.[8] at $\sqrt{s} = 27.4$ is given in Fig. 4 for several values of Q with the predicted normalization. The presence of transverse momentum fluctuations, due to the (small) k_T's present in the initial wave functions, will slightly flatten the theoretical curves. Note that the mass bins for different Q values are not constant in width.

$\underline{Q_L \neq 0}$: A comparison with the data of Anderson et al.[7] at $\sqrt{s} = 20.6$, is given in Fig. 5 for two Q bins. The theoretical predictions were integrated over the range $x_F > 0.15$ to correspond to the experimental situation and were arbitrarily normalized. As remarked before, our model is not complete enough to fit the normalization at the lowest Q where the normal vector mesons are important, while the upper mass bin includes effects of ψ/J production. The fit suggests that this particle is also produced by the same mechanism as the photon. Note that this plot differs by a factor of Q_0 from that of Fig. 3 and that the t-u symmetry of R is equivalent to a $Q_L \rightarrow -Q_L$ symmetry for incident proton beams. For Q ~ 2 GeV, the predicted normalization is in agreement with the data using the modified structure functions mentioned earlier.

For both regions of Q_L, the model fits the Q_T distribution very well except at very small Q_T where the effects of the transverse momentum fluctuations in the initial state will be most sharply seen. Again, these fluctuations will lower the theoretical curve at small Q_T, $Q_T \lesssim 400$ MeV/c (we estimate ≈30%), but will have little effect at larger transverse momentum values.

C. Longitudinal Distribution

The y-distribution of the meson-quark model as compared with the data of Ref. 8 is given in Fig. 6 with the predicted normalization. Note the shape of the y-distribution as Q increases.

The x_F distribution is compared with the data of Anderson et al.,[7] in Fig. 7 for two mass bins. The agreement of the shape is reasonable. These curves have been normalized to the data for the reasons given earlier.

D. $\langle Q_T \rangle$

In this paragraph, the average transverse momentum will be computed as a function of Q. This is not as sensitive a test of the model as it is of the Q_T distribution used by the experimentalists to extract $\langle Q_T \rangle$, but it is interesting since the effects of initial state fluctuations in k_T can be easily estimated. Since these effects are essentially uncorrelated and small, we can sum their squares and find, very roughly,

$$\langle Q_T^{total} \rangle \simeq \left[\langle Q_T \rangle^2 + \langle k_\pi^2 \rangle + \langle k_q^2 \rangle \right]^{1/2}$$

$$\simeq \left[\langle Q_T \rangle^2 + 0.3 \right]^{1/2} \tag{13}$$

for $\langle k_\pi \rangle = \langle k_q \rangle \sim 330$ MeV/c, where $\langle Q_T \rangle$ is computed from our previous formulae. The results are plotted in Fig. 8. The lower curve is calculated for the data of Ref. 7. The upper two curves, the solid curve is $\langle Q_T \rangle$ and the dashed curve includes the fluctuation effects of Eq. (13), are computed at the higher energy and are to be compared with the data of Ref. 8 and Kluberg et al.[9] Note that $\langle Q_T \rangle$ increases with Q but saturates for $Q \gtrsim 4$ GeV/c. It appears that our transverse momentum distributions (see Fig. 4) fit the data better than our $\langle Q_T \rangle$ values. The averages in Fig. 8 should be taken with a grain of salt—they are very sensitive to the assumed form of the Q_T distribution.

The $\langle Q_T \rangle$ curve does not in general saturate at the value of M. For M=1, they are almost equal in the present energy range, but for a smaller M value, $\langle Q_T \rangle$ exceeds M by a substantial amount. For example, for M=0.5, $\langle Q_T \rangle \sim 0.66$, and $\langle Q_T^{total} \rangle \sim 0.88$. However, this mass is much too small to fit the large P_T data; the smallest fitted value we have seen is M~0.85.

It is interesting to note that the increase in the $\langle Q_T \rangle$ which sets the Q_T scale is also observed in large P_T experiments. The mass scale used to fit the data increases with the mass of the detected particle. This is consistent with a common type of mechanism for the production of large P_T particles and massive photons.

V. DISCUSSION

From the comparisons in the previous section, the meson-quark model is seen to provide a good representation of the experimental data. We emphasize that the only parameters in the model were determined by fitting other data, principally large P_T production of mesons and inelastic neutrino scattering. The fact that the overall normalization was consistent between the D-Y model, using standard quark charges and distribution functions, and large P_T meson production is strong evidence in favor of the M-q model.

It is a simple matter to make predictions for other beams, such as pion and photon, by using the appropriate distribution functions. Results for these calculations will be given later. Suffice it to say at this point that the predictions of our model are much less sensitive to the presence of valence antiquarks in the initial state than is the D-Y model. In our model, pion beams and proton beams look very similar (except for the effects of the different values of g_M, g_q and $g_{\bar{q}}$ and leading particle effects in the fragmentation region of the pion).

The meson-quark model makes several predictions for the final state which can be checked experimentally. The large Q_T of the photon is balanced by a recoil quark. Thus the final state jet should look the same as those seen at SPEAR, in electron scattering, and in large P_T meson production. The angular dependence of the balancing "jet" is determined in terms of the distribution functions and the angular distribution for $Mq \rightarrow \gamma q$ (the correct angular dependence will have to be computed with spin one-half quarks and not the scalar model used here). In general, we expect that the π^+/π^- ratio in the jet will increase as a function of Q_T.

Another prediction of the model is that for any incident beam, the transverse momentum distribution falls as Q_T^{-6} for $Q_T \gg Q$ and Q_T^{-4} for $Q_T \ll Q$. Finally, we note that since massive lepton pairs and large P_T mesons are produced by a very similar mechanism, namely meson-quark scattering, the ratio of prompt single leptons to pions, ℓ/π, is expected to be quite constant. However, since the former is predicted to fall as Q_T^{-6} and the latter as Q_T^{-8}, the ratio should rise as a function of Q_T. This trend is observed in the data.[4] The width of the Q_T distribution will aid the theoretical calculations in getting a sufficient number large transverse momentum prompt leptons to fit the data.[5]

Let us contrast our model with that of Drell-Yan. In the meson-quark model used here, the photons are assumed to arise from the interaction of the beam with virtual mesons in the cloud of the target (or vice versa) in an inverse photoproduction process. Inside this process, there are graphs that can be identified as quark pair annihilation, the basic D-Y process. Since our model explicitly focuses upon a scattering process, the generation of large Q_T is to be expected with a scale set by Q^2 and M^2. We predict a Q_T^{-6} falloff for $Q_T > Q$, and an $\langle Q_T \rangle$ that depends on Q and a mass parameter M that is characteristic of all large P_T reactions. For small Q_T, it is not possible to freely "boil off" heavy particles, so that the massive photon distribution does not have the sharp (exponential) peak at small P_T that characterizes the pion spectra, for example. The average transverse momentum in the initial state plays a minor role in our model.

In conclusion, this model agrees very well with the experimental data from proton beams using no new parameters. All the parameters are determined in terms of the measured antiquark distribution, the large transverse momentum production of mesons, and the dimensional counting rules.[15, 17] A consistency check between the normalization of the two input measurements is satisfied. Further tests of the model will involve other incident beams, extension of the measurements throughout the Peyrou plot, and detailed tests of final state correlations.

REFERENCES

1. J. H. Christensen et al., Phys. Rev. Letters 25, 316 (1970), and Phys. Rev. D 8, 2016 (1973).
2. S. D. Drell and T. M. Yan, Phys. Rev. Letters 25, 316 (1970), and Ann. Phys. (N.Y.) 66, 578 (1971).
3. J. W. Cronin, Lectures presented at the International School of Subnuclear Physics, Erice, July, 1976.
4. See the excellent review by P. A. Piroué, Princeton preprint, presented to the 1976 Particles and Fields Conference, BNL, October, 1976. Further references are contained therein.
5. For both pair and single yield see M. Duong-van, Phys. Letters 60B, 287 (1976) and SLAC-PUB-1604 (1975). For the pair yield only, see also G. Chu and J. F. Gunion, Phys. Rev. D 10, 3672 (1974), and G. R. Farrar, Nucl. Phys. B77, 429 (1974).
6. M. Binkley et al., Phys. Rev. Letters 37, 574 (1976).
7. K. J. Anderson et al., Phys. Rev. Letters 37, 799 (1976).
8. D. C. Hom et al., Phys. Rev. Letters 37, 1374 (1976).
9. L. Kluberg et al., Phys. Rev. Letters 37, 1451 (1976).
10. M. Duong-van, SLAC-PUB-1819 (1976). D. Soper, Princeton preprint (1976). J. F. Gunion, U. C. Davis preprint (1976). P. Landshoff, DAMTP preprint 76/23 (1976). W. Caswell and R. Horgan (private communication). See also E. M. Levin and M. G. Ryskin, Leningrad preprint INP (1975), submitted to Zh. Eksp. Teor. Fiz., for a discussion of the effects of large transverse momenta in the hadron wave function.
11. C. T. Sachrajda and R. Blankenbecler, Phys. Rev. D 12, 3624 (1975). See also Stanford Linear Accelerator Center preprint SLAC-PUB-1531 (1975) (unpublished).

12. M. Fontannaz, Orsay preprint LPTHE 75/29 (1975). Our model differs from the one discussed here. This model does not contain the Drell-Yan contribution in the appropriate limit but does have a broad Q_T distribution.

13. R. Blankenbecler, S. J. Brodsky and J. F. Gunion, Phys. Rev. D 6, 2652 (1972). See also D. Sivers, S. J. Brodsky and R. Blankenbecler, Physics Reports 23C, No. 1 (1976).

14. C. T. Sachrajda and R. Blankenbecler (unpublished) but used in the calculations of M. Duong-van, Refs. 5 and 10. For an application of this type of wave function to relativistic heavy ion reactions, see I. Schmidt and R. Blankenbecler, Stanford Linear Accelerator Center preprint, "Relativistic Interactions Between Nuclei", SLAC-PUB-1881 (1977).

15. R. Blankenbecler and S. J. Brodsky, Phys. Rev. D 10, 2973 (1974).

16. This assumption is consistent with a study of the antiquark distribution functions in weak, electromagnetic and strong reactions by T. Goldman and G. West (private communication), to be published.

17. S. J. Brodsky and G. R. Farrar, Phys. Rev. Letters 31, 1153 (1973); Phys. Rev. D 11, 1309 (1975).

18. J. F. Gunion, S. J. Brodsky and R. Blankenbecler (to be published).

FIGURE CAPTIONS

1. General diagram for massive pair production in hard scattering models. Particle labels are used in the text.

2. Leading diagram for the basic inverse photoproduction process. Both u- and s-pole terms are needed, and the u-pole clearly has pair annihilation contributions.

3. The predictions of the M-q model and the Drell-Yan model for the cross section at y=0 compared to the data of Kluberg et al. and Hom et al.

4. The predicted transverse momentum distribution of the M-q model compared to the data of Hom et al. for various mass bins.

5. The predicted transverse momentum distributions, normalized to and compared to the data of Anderson et al. at 150 GeV/c.

6. The predicted y distributions are compared to the data of Hom et al. for several mass ranges.

7. The predicted Feynman-x distributions normalized as in Fig. 5 are given and compared to the data of Anderson et al.

8. The average transverse momentum from the M-q model are given at two energies and x ranges and compared to the corresponding data. The solid curves are without fluctuation effects; the dashed curve is an estimate of the effects of initial state momentum fluctuations on the 400 GeV curve.

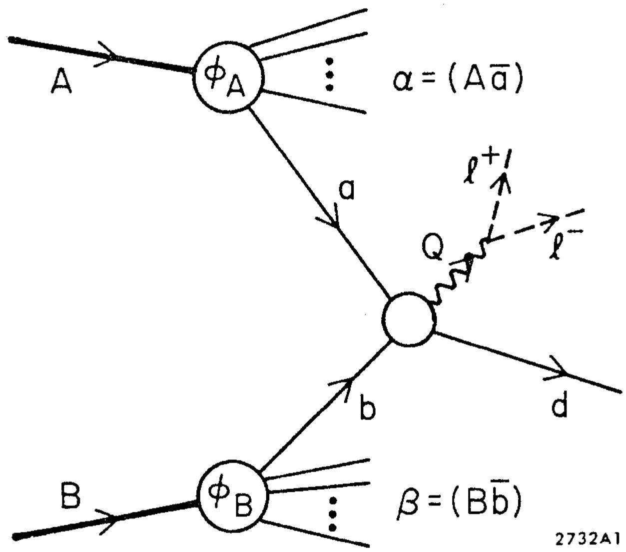

Fig. 1

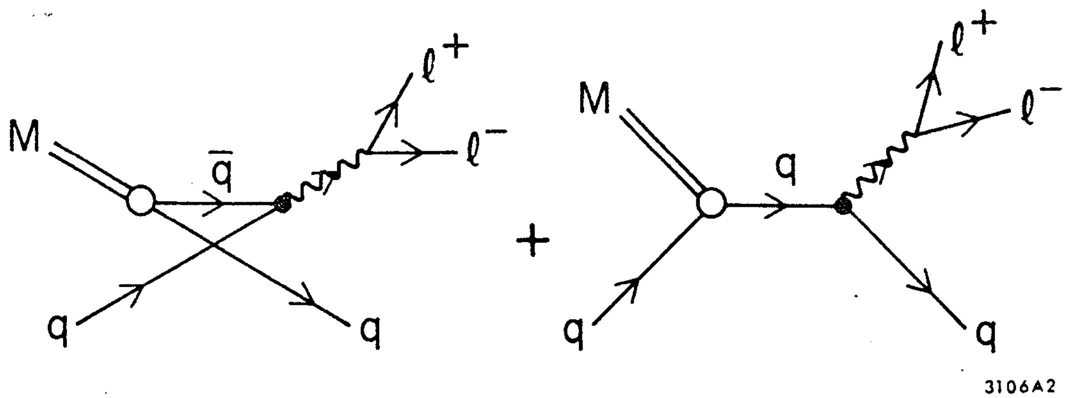

Fig. 2

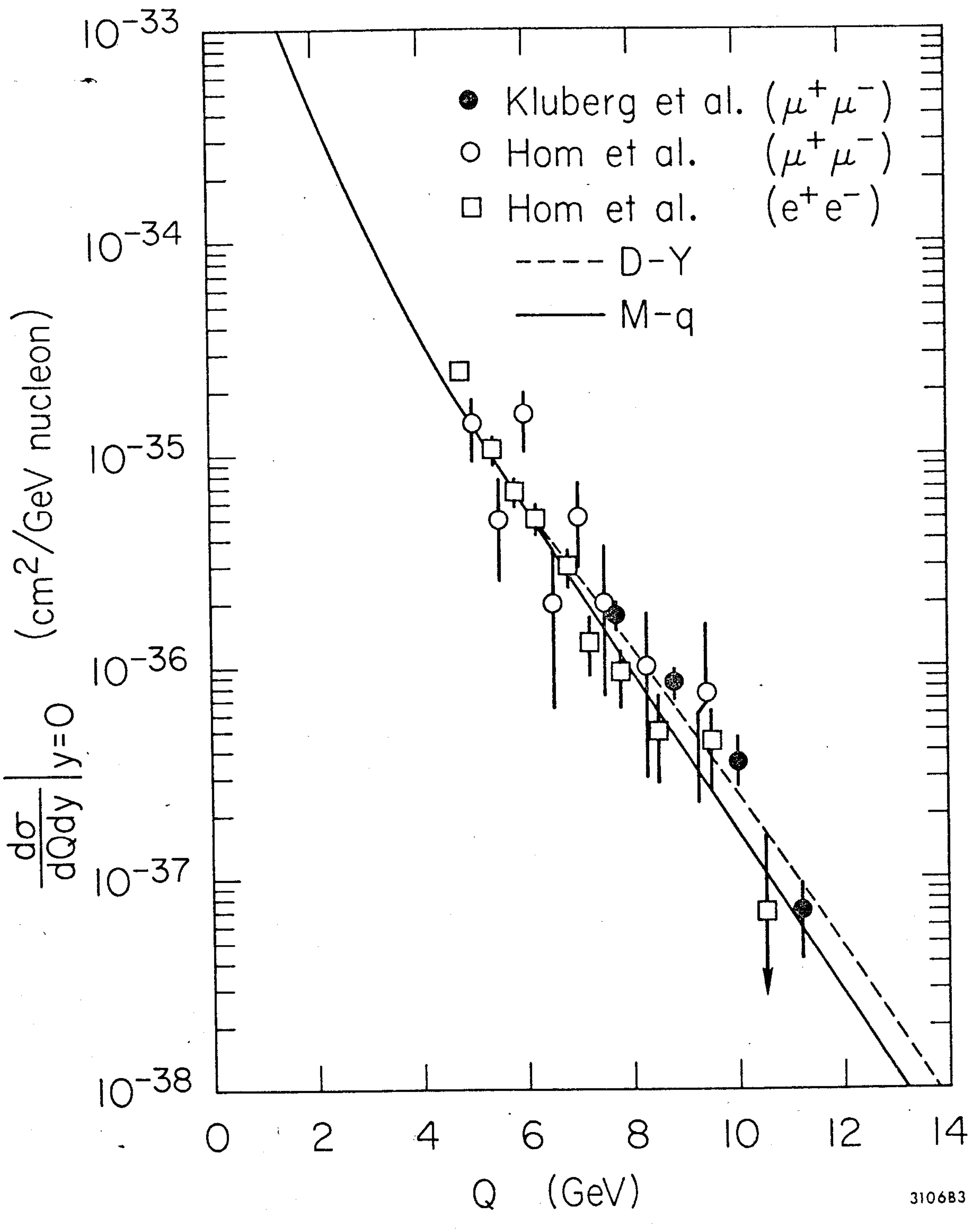

10^{-33}
10^{-34}
10^{-35}
10^{-36}
10^{-37}
10^{-38}
$\left.\frac{d\sigma}{dQdy}\right|_{y=0}$ (cm^2/GeV nucleon)
Kluberg et al. ($\mu^+\mu^-$)
Hom et al. ($\mu^+\mu^-$)
Hom et al. (e^+e^-)
D-Y
M-q
0
2
4
6
8
10
12
14
Q (GeV)
3106B3

Fig. 3

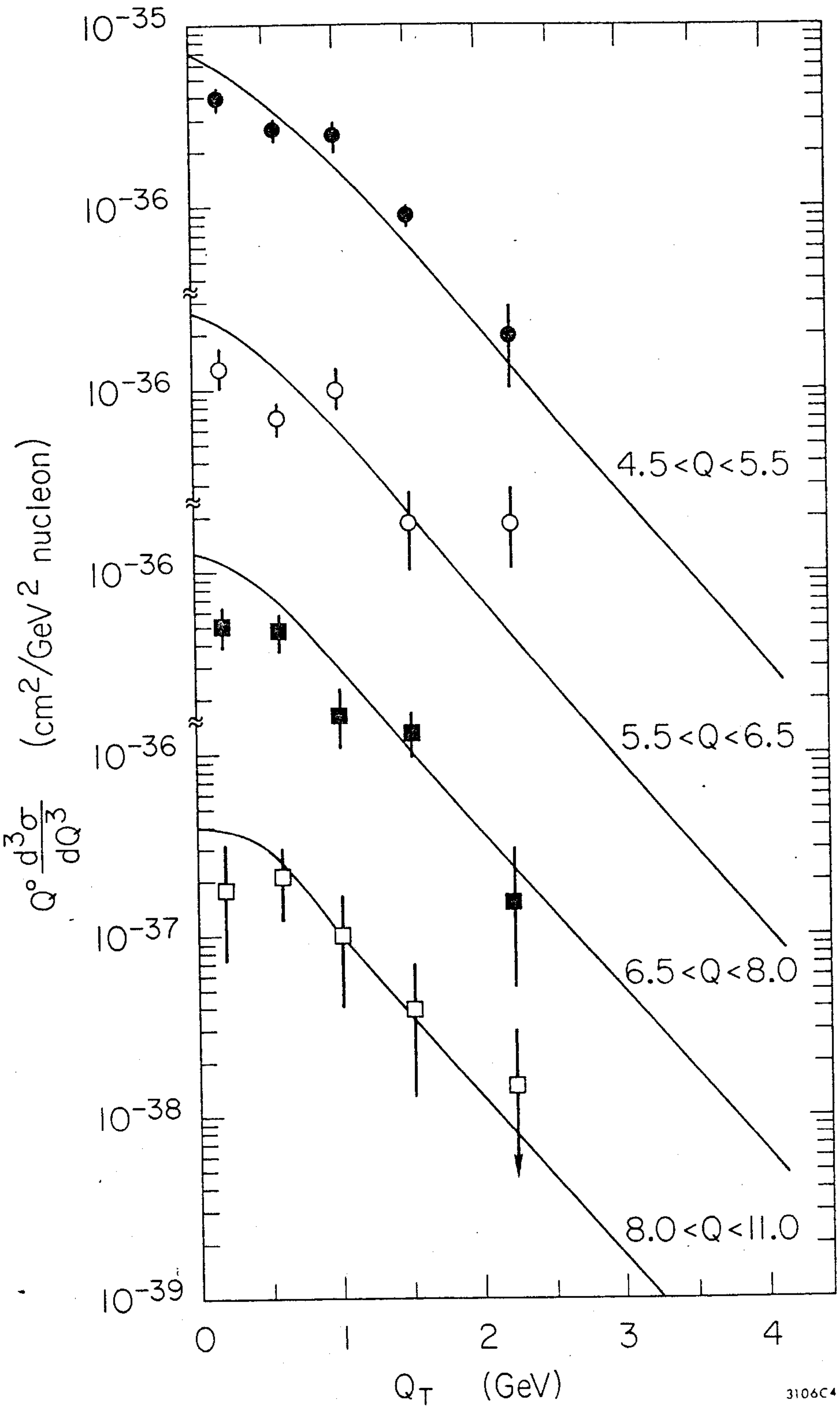

10^{-35}
10^{-36}
10^{-36}
10^{-36}
10^{-36}
10^{-37}
10^{-38}
10^{-39}
$Q^{\circ}\frac{d^3\sigma}{dQ^3}$ (cm^2/GeV^2 nucleon)
4.5<Q<5.5
5.5<Q<6.5
6.5<Q<8.0
8.0<Q<11.0
0
1
2
3
4
Q_T (GeV)
3106C4

Fig. 4

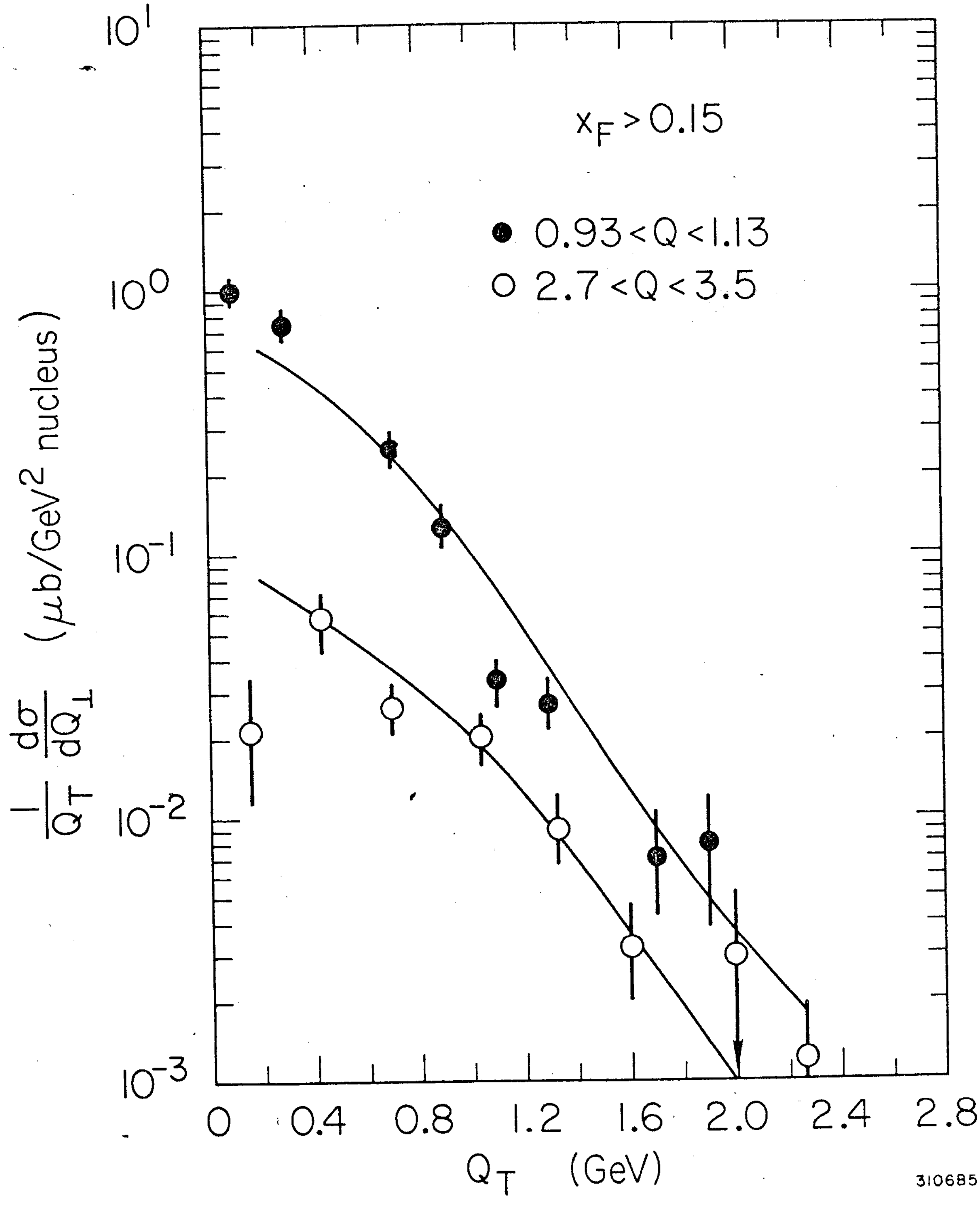

$x_F > 0.15$
● $0.93 < Q < 1.13$
○ $2.7 < Q < 3.5$
$\frac{1}{Q_T}\frac{d\sigma}{dQ_T}$ (μb/GeV^2 nucleus)
10^1
10^0
10^{-1}
10^{-2}
10^{-3}
0
0.4
0.8
1.2
1.6
2.0
2.4
2.8
Q_T (GeV)
310685

Fig. 5

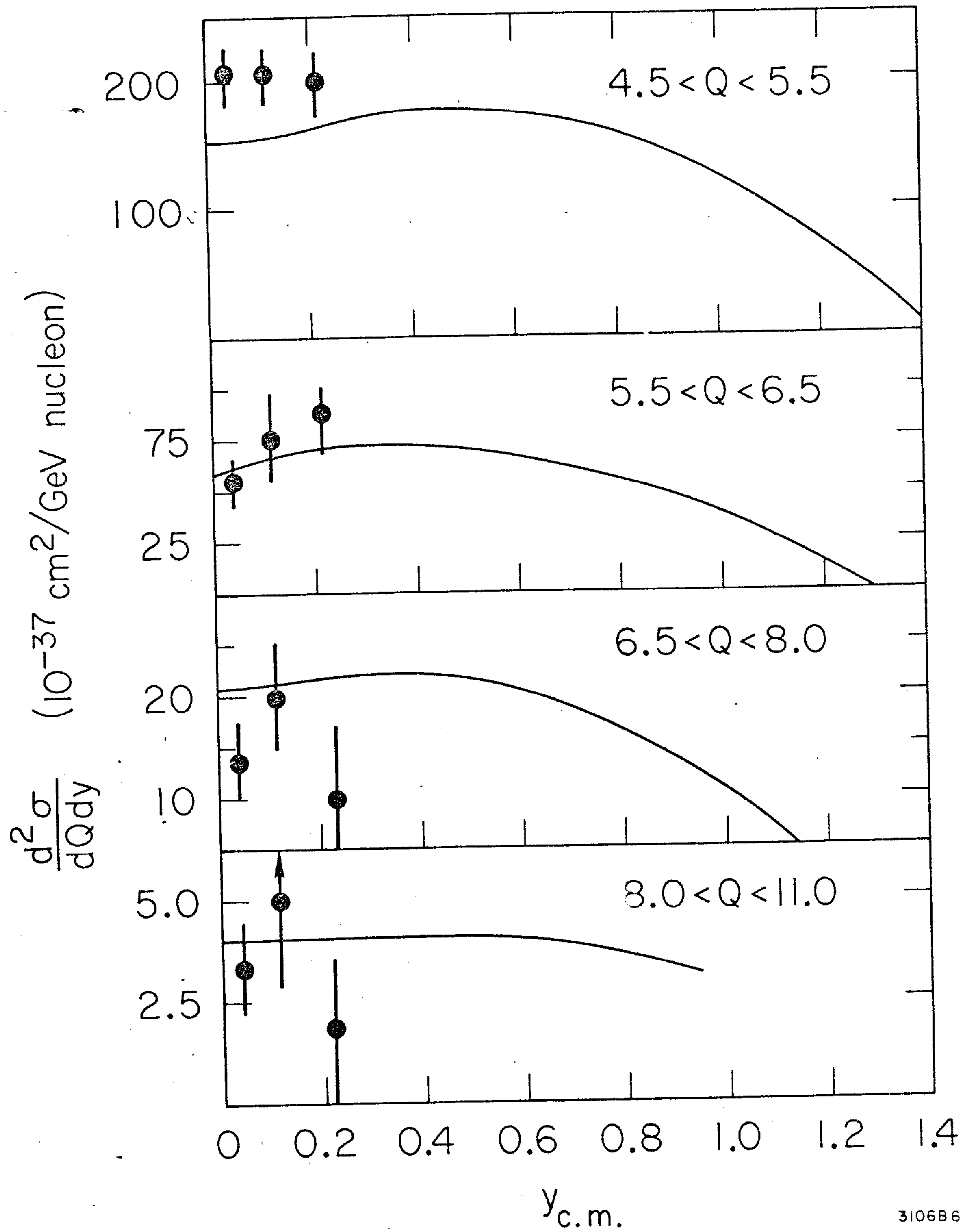

4.5<Q<5.5
5.5<Q<6.5
6.5<Q<8.0
8.0<Q<11.0
200
100
75
25
20
10
5.0
2.5
$\frac{d^2\sigma}{dQdy}$ (10^{-37} cm^2/GeV nucleon)
0
0.2
0.4
0.6
0.8
1.0
1.2
1.4
$y_{c.m.}$
3106B6

Fig. 6

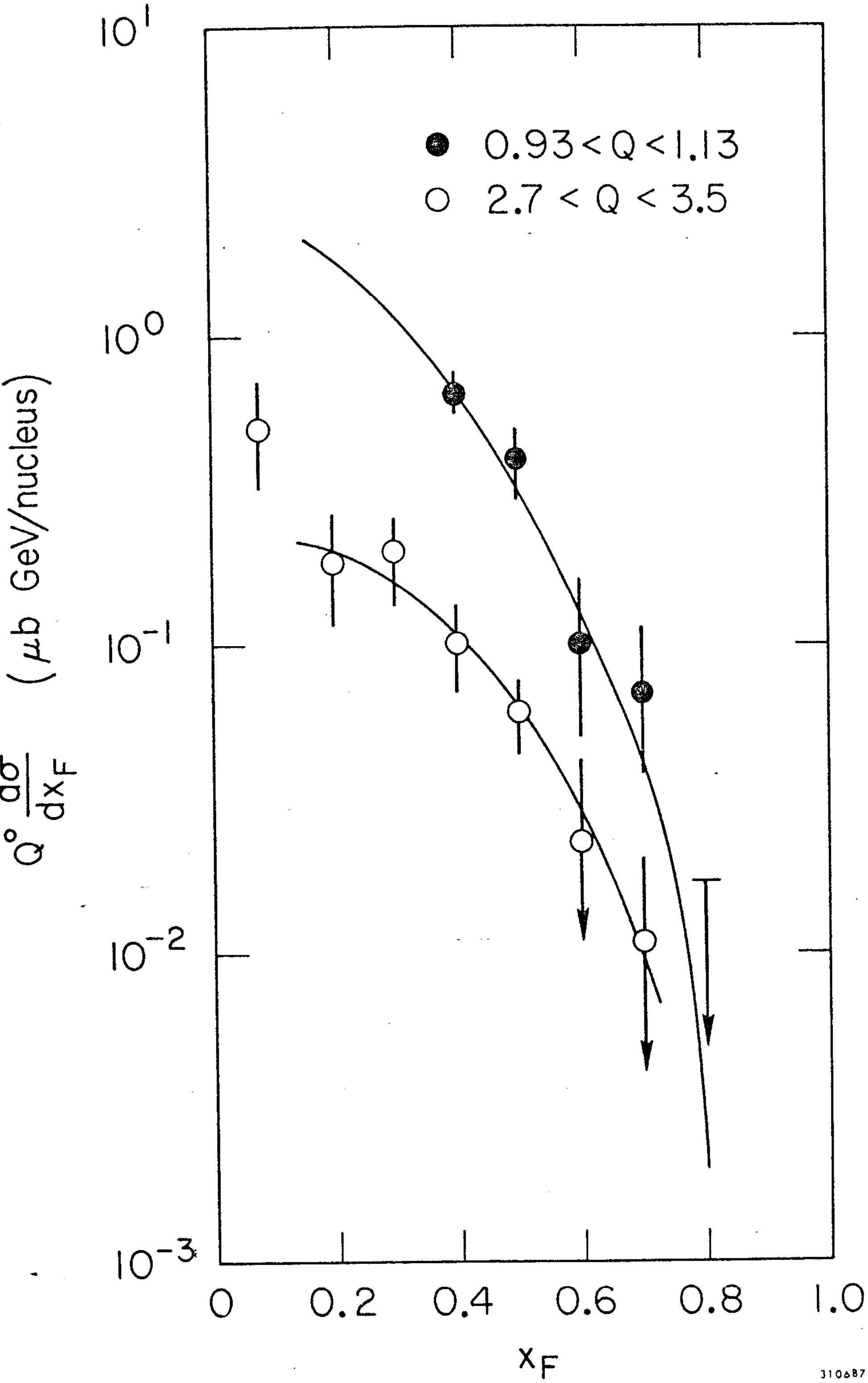

0.93 < Q < 1.13
2.7 < Q < 3.5
10^1
10^0
10^{-1}
10^{-2}
10^{-3}
$Q^\circ \frac{d\sigma}{dx_F}$ (μb GeV/nucleus)
0
0.2
0.4
0.6
0.8
1.0
x_F
310687

Fig. 7

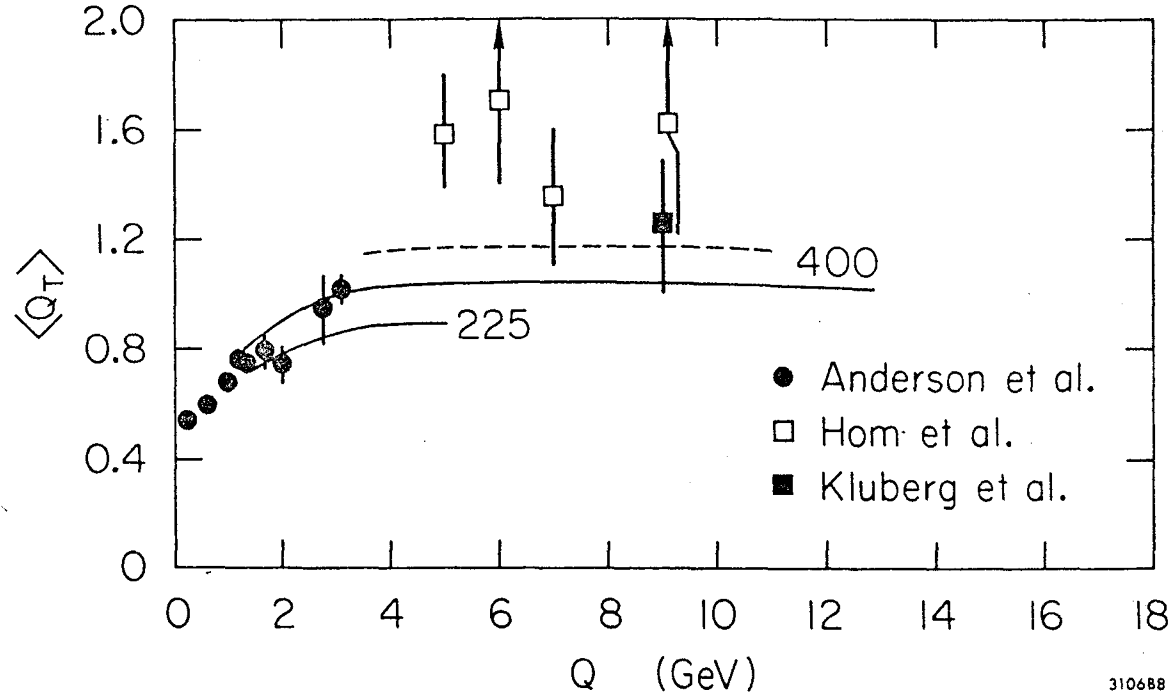

2.0
1.6
1.2
0.8
0.4
0
⟨Q_T⟩
0
2
4
6
8
10
12
14
16
18
Q (GeV)
400
225
Anderson et al.
Hom et al.
Kluberg et al.
3106B8

Fig. 8